





## Investigating the neural correlates of stroop effect using the multilayer perceptron neural network

Elif Uğurgöl<sup>1</sup>,  Miray Altinkaynak<sup>2</sup>,  Demet Yeşilbaş<sup>1</sup>,  Turgay Batbat<sup>3</sup>,  Aysegül Güven<sup>3,4</sup>,  
Esra Demirci<sup>5</sup>,  Meltem İzzetoğlu<sup>6</sup>,  Nazan Dolu<sup>7</sup> 

<sup>1</sup>Department of Biomedical Engineering, Graduate School of Natural and Applied Sciences, Erciyes University, Türkiye

<sup>2</sup>Department of Biomedical Engineering, Neurophotonics Center, Boston University, Massachusetts, USA

<sup>3</sup>Department of Biomedical Engineering, Engineering Faculty, Erciyes University, Türkiye

<sup>4</sup>Clinical Engineering Research and Implementation Center, Erciyes University, Türkiye

<sup>5</sup>Department of Child and Adolescent Psychiatry, Medical Faculty, Erciyes University, Türkiye

<sup>6</sup>Electrical and Computer Engineering Department, Villanova University, USA

<sup>7</sup>Department of Physiology, Medical Faculty, Medipol University, Türkiye

### ABSTRACT


**Aim:** The Stroop task, specifically related to semantic conflict processing, is one of the most common cognitive tests examining executive functions. This study aimed to investigate neural correlates of the Stroop interference effect by means of simultaneous electroencephalography (EEG) and functional near infrared spectroscopy (fNIRS) measurements using a machine learning approach.

**Methods:** A total of forty-five healthy male university students were included in the study. We measured brain activation with EEG/fNIRS systems during the color-word matching Stroop task. Linear and non-linear dynamics of EEG were computed over five frequency sub-bands. fNIRS analysis was conducted with a general linear model. We combined features from both modalities and employed the Multilayer Perceptron (MLP) algorithm to classify incongruent and neutral trials. The Stroop effect in the subregions of the prefrontal cortex was also investigated using statistical analyses.

**Results:** The results indicated that brain activation due to Stroop interference increased with incongruent stimuli, particularly in the right dorsolateral prefrontal cortex. The Stroop effect was associated with the fractal dimension and power spectral density of EEG. There was a significantly longer reaction time and more task error with incongruent stimuli than neutral trials. MLP classified incongruent and neutral trials with an accuracy rate of 73.3%.

**Conclusions:** This study is the first to examine the Stroop effect using a multimodal EEG/fNIRS system and machine learning approach. Our study revealed that a hybrid EEG/fNIRS system is an effective neuroimaging tool to study neural correlates of Stroop interference. These findings could be used in future neurological and psychiatric research.

**Key words:** Stroop effect, electroencephalography, functional near infrared spectroscopy, multilayer perceptron.

 Dr. Miray Altinkaynak, Ph.D.  
Biomedical Engineering, Neurophotonics Center  
College of Engineering, Boston University  
610 Commonwealth Avenue, Boston, MA 02215, USA  
E-mail: [maltinka@bu.edu](mailto:maltinka@bu.edu), [em.miray@gmail.com](mailto:em.miray@gmail.com)

Received: 2024-05-06 / Revisions: 2024-07-28

Accepted: 2024-09-03 / Published: 2024-09-30

## 1. Introduction

The executive functions of the brain include high-order cognitive processes such as planning, decision-making, and attentional control, which regulates thoughts and behaviors [1, 2]. The regulation of executive functions within the context of cognitive processes is called cognitive control. Therefore, observing different cognitive processes enhances our comprehension and insight into brain functions. Cognitive control can be observed more clearly in situations where the brain needs to respond more prominently to one stimulus over others [3, 4].

There have been various cognitive tests to evaluate executive functions. Stroop task has been referred to as a gold standard for identifying selective attention and inhibition, and it is commonly used for experimental and clinical purposes. The classic Stroop task, developed by J. R. Stroop in 1935, is based on the color-word conflict [5]. The Stroop effect arises from this conflict and reflects the extra effort exerted by the brain when the color of a word does not match the color it represents [6, 7]. The classic Stroop test includes three main types of stimuli: congruent, incongruent, and neutral stimuli. In congruent stimuli, the words are written in the color they represent, while in incongruent stimuli, the word is written in a color different from its meaning (e.g., the word "RED" written in yellow). Neutral stimuli do not semantically convey either conflicting or matching conditions. The distinction between the brain's response to incongruent stimuli and neutral stimuli is referred to the Stroop interference effect [8, 9]. The Stroop effect is prominently observed through differences in reaction time (RT) across diverse types of stimuli. RT refers to the duration between the presentation of a stimulus and the subject's response. One of the more consistent findings in Stroop effect research is that reaction

times to incongruent stimuli are typically longer compared to those for congruent or neutral stimuli, attributed to the interference effect [10]. In this study we examined reaction times for each stimulus and computed task errors to analyze behavioral data.

Stroop interference effect has been investigated in various neuroimaging studies, including magnetoencephalography (MEG) [11], functional magnetic resonance imaging (fMRI) [12], positron emission tomography (PET) [13], and it has been associated with various measurements [10, 14-17]. Electroencephalography (EEG), known for its high temporal resolution, has been widely used to investigate brain dynamics during the Stroop test [18, 19]. The Stroop effect was associated with increased theta activity [15] and decreased P3 and N4 amplitude. Recently Sobhani et al. [20] highlighted the importance of nonlinear EEG features alongside linear features when investigating the Stroop effect. They reported increased fractal dimension (FD) and entropy values, especially in the occipital region, during the Stroop task compared to the resting state.

In addition to electrophysiological methods, hemodynamic changes of the brain are also widely investigated to identify neural correlates of the Stroop effect. Recently, Smith et al. [12] demonstrated the association between brain activity and behavioral performance during the Stroop task with fMRI. A meta-analysis of fMRI studies conducted with the Stroop task revealed increased brain activation due to Stroop effect especially in frontal areas [21]. Similar to fMRI, functional near-infrared spectroscopy (fNIRS) is a non-invasive optical technique that detects neural activity through changes in blood flow. The key difference is that fNIRS is more cost-effective and portable, allowing it to be used as a wearable device. fNIRS has been utilized widely to assess cognitive function over the last two

decades [22]. This method measures the level of oxygenation in the brain based on hemodynamic changes [23]. Several fNIRS studies conducted on healthy adults have demonstrated increased activation, particularly in the prefrontal region, when presented with incongruent stimuli compared to neutral stimuli [8, 24].

In recent years, the integration of neuroimaging techniques has been commonly employed to provide comprehensive information [25]. Li et al. [26] measured brain activation using a wearable system that integrates EEG and fNIRS techniques. Chen et al. [27] collected EEG and fNIRS data while participants performed the Stroop task to investigate the neural correlates of attention and decision-making processes. Their findings revealed a significant decrease in neural activation in response to incongruent stimuli, offering valuable insights into the neural mechanisms underlying cognitive conflict. This current study combined EEG and fNIRS modalities to investigate the Stroop effect. Linear and nonlinear brain dynamics of EEG and hemodynamic features derived from fNIRS were combined, and selected features were applied to the MLP algorithm to provide an objective, comprehensive approach to investigating the Stroop effect. MLP is a supervised learning algorithm that uses nonlinear activation functions, enabling it to learn complex relationships within the data. This is the first study to examine the Stroop effect using a multimodal EEG/fNIRS system and machine learning approach.

## 2. Materials and methods

### 2.1. Participants

Forty-five healthy male students aged between 18-23 years, with a mean age of 20.98 ( $\pm 1.59$ ) were included in the study. Participants underwent a clinical evaluation by a specialized

psychiatrist. All participants were native Turkish speakers, had normal hearing and normal or corrected-to-normal visual functions, had no history of neurological or psychiatric disorders, and were right-handed. The ethical protocols were per the Helsinki Declaration and were approved by Erciyes University Clinical Research Ethics Committee with the number 2023/65. Informed consent was obtained from all subjects before enrollment.

### 2.2. Procedure

The data was collected in a Faraday-cage designed for recording physiological signals at the Clinical Engineering Research and Application Center of Erciyes University. Participants were seated in comfortably chairs, positioned 130 cm away from the computer screen. Participants were instructed to keep their eyes open, not move, and press response buttons when they encounter specified event. Data collection was begun after participants became familiar with the task. EEG and fNIRS data were recorded simultaneously. Behavioral data were automatically recorded via a setup designed using Arduino.

In this study, the classic Stroop task was employed and measurements were conducted during congruent, incongruent, and neutral trials [5, 28]. Since all participants were native Turkish speakers, the Turkish version of the Stroop task was utilized. In Turkish, "KIRMIZI" means red, "SARI" means yellow, "MAVİ" means blue, and "YEŞİL" means green, and the Stroop task was administered based on these four colors [29]. During the Stroop task, as seen in Figure 1, two rows of letters appeared on a black screen and participants were asked to respond to the trials by pressing buttons in their right and left hands. In congruent stimuli the color matched with the word's, meaning while in incongruent stimuli, the color name contradicted the word's color. In neutral stimuli consisted of "XXXX" printed in

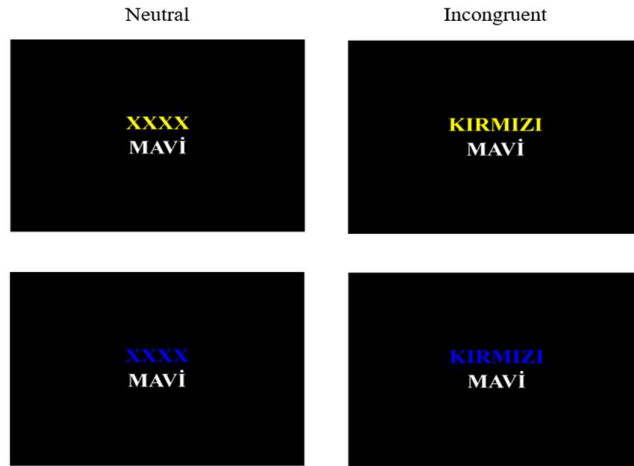


**Figure 1.** Examples of trials for the neutral and incongruent stimuli of the Stroop color-word task.

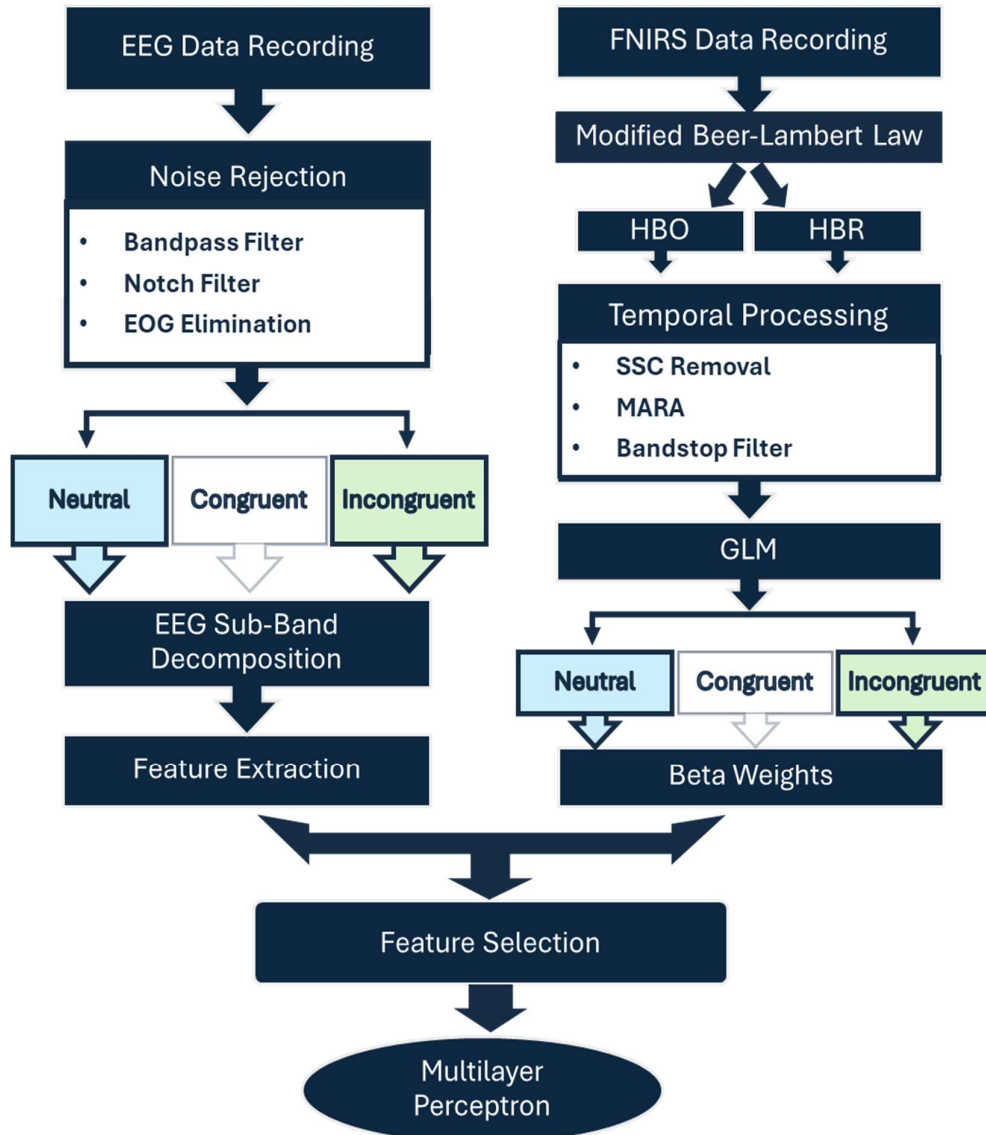


**Figure 2.** The flowchart of the study.

assorted colors in the top row, with color words presented in the bottom row. If the color of the top statement matched the color name in the bottom statement, it was labeled as "Yes-response" and the participants were asked to press right button in that case; otherwise, it was labeled as "No-response", and the participants were instructed to press the left button. A total of 150 stimuli comprising 50 congruent, 50 incongruent, and 50 neutral stimuli were presented in a random order with an inter-stimulus interval of 1650 ms. The study was proceeded on incongruent and neutral stimuli response to investigate Stroop interference effect. The flowchart of the study is presented in Figure 2. Details of each step are presented in the following sections.

### 2.3. Data Acquisition

#### 2.3.1. EEG data acquisition:

The EEG signals were recorded using the EBNeuro BE-Light 36 EEG device. Signals from 17 channels (F7, F3, Fz, F4, F8, T3, C3, Cz, C4, T4, T5, P3, Pz, P4, T6, O1, and O2) were obtained using a cap fitted with Ag/AgCl electrodes arranged according to the international 10-20 system. Additionally, three electrodes were used to record Electrooculogram (EOG) signals to eliminate eye movements [29,30]. For both the EEG and EOG channels, the reference electrode was positioned on the left mastoid, while the ground electrode was placed on the right mastoid. The impedance of the electrodes was maintained below 10 k $\Omega$ , and the data was recorded at a sampling rate of 512 Hz.

#### 2.3.2. fNIRS data acquisition:

fNIRS signals were recorded with the BIOPAC fNIRS Model 203c (fNIR Devices, LLC, Potomac, MD, USA) device. The system measures changes in oxygenated hemoglobin (HbO) and deoxygenated hemoglobin (HbR) using two different wavelengths: 850 nm and 730 nm, respectively. The fNIRS band has 4 NIR

light sources, 10 long-channel detectors and 2 short-channel detectors. This set-up comprised 16 long-distance optodes at 2.5 cm away from the light source and 2 short distance optodes at 1 cm away from the detectors, providing a total of 18 channels for recording. The sampling rate was 10 Hz. Figure 3 shows experimental design of the study. EEG, fNIRS and EOG signals were recorded simultaneously.

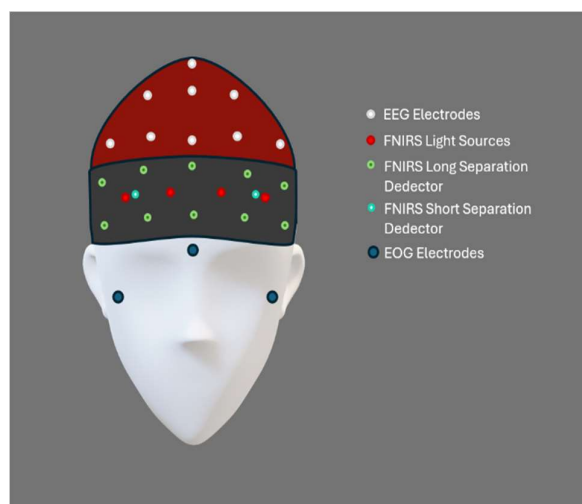


**Figure 3.** Experimental design of the study.

### 2.4. Signal Processing

#### 2.4.1. EEG Signal Processing:

EEG processing was performed using EEGLab v2023.1 within the MATLAB environment (Matlab 2022a) [31]. Initially, bandpass filtering (0.5-60 Hz) and a 50 Hz Notch filter were applied, then independent component analysis (ICA) was employed to remove artifacts arising from eye movements [32]. After pre-processing, EEG responses were grouped according to congruent, incongruent, and neutral conditions. Then, EEG signals were decomposed into five frequency bands using a four-level dB5 (Daubechies 5) wavelet function: gamma (30-40 Hz), beta (12.5-30 Hz), alpha (7.5-12.5 Hz), theta (4-7.5 Hz), and delta (<4 Hz). Each channel's sub-bands were then evaluated for further analysis. Various linear and non-linear features

were calculated to investigate the Stroop effect for each EEG sub-band (see Table 1). The brief description of features are presented below:

**Table 1.** Features calculated from EEG sub-bands.

EEG Sub-bant features
1. Mean
2. Standart Deviation
3. Fractal Dimension
4. Shannon Entropy
5. Hlbert Entropy
6. Skewness
7. Hurst Exponent
8. Harmonic Distortion
9. Lyapunov Exponent
10. Power Spectral Density Features

**2.4.1.1. Fractal Dimension:** Fractal dimension is a measure of EEG complexity and it is associated with brain activation [33]. One of the most commonly used methods for this calculation is Katz's approach, which is directly applied to two-dimensional time series. The algorithm for calculating Katz's fractal dimension is shown in Eq. 1:

$$FD = \frac{\ln \frac{L}{a}}{\ln \frac{d}{a}} \quad (1)$$

where d represents the longest distance to the origin, L is the total length of the time series and a is the average distance between successive samples in the time series.

**2.4.1.2. Shannon Entropy:** Shannon entropy indicates the uncertainty of the signal and has a probability-based mathematical framework. This framework relies on the logarithmic average of the probabilities of events occurring as seen in Eq. 2 [34]:

$$E(n) = - \sum_{i=0}^{N-1} P_i^2 [n] \log_2(P_i^2 [n]) \quad (2)$$

In the equation, the value of  $P_i^2 [n]$  represents the probability, while the value of N denotes the sample size.

**2.4.1.3. Hilbert Entropy:** Hilbert entropy measures the randomness or unpredictability of the phase variations over time [35]. The Hilbert entropy is defined by the Eq. 3:

$$y(t) = \frac{1}{\pi} P \int_{-\infty}^{\infty} \frac{x(\tau)}{t - \tau} d\tau \quad (3)$$

where P denotes principal values of Cauchy and  $\tau$  is the integral variable.

**2.4.1.4. Skewness:** Skewness indicates the deviation of the data from a normal distribution [36]. It is calculated as shown in Eq. 4, where S represents the skewness value, x is the time series,  $\mu$  is the mean of the time series, E denotes the expected value of the random variable, and  $\sigma$  is the standard deviation of the time series.

$$S = \frac{E(x - \mu)^3}{\sigma^3} \quad (4)$$

**2.4.1.5. Harmonic Distortion:** Harmonic distortion quantifies the level of deviation from a pure sinusoidal waveform in a signal [37]. It is calculated as shown in Eq. 5, where  $V_1$  represents the root mean square of the lowest frequency component of the signal, and  $V_n$  represents the root mean square of all other components.

$$HD = \frac{\sqrt{\sum_{n=2}^{\infty} V_n^2}}{V_1} \%100 \quad (5)$$

**2.4.1.6. Hurst Exponent:** Hurst exponent is a measure of interdependence among samples in a time series [38]. It is calculated as in Eq. 6:

$$H = \frac{\log \left( \frac{R}{S} \right)}{\log(N)} \quad (6)$$

where N is the window length, S is the standard deviation and R is the cumulative standard deviation.

**2.4.1.7. Lyapunov Exponents:** Lyapunov exponents indicates the system's sensitivity to initial



conditions and those are crucial for understanding chaotic behavior of the signal [39]. As shown in Eq. 7, the distances of the nearest points in the direction I at times 0 and t in phase space are denoted by  $\|\delta x_i(0)\|$  and  $\|\delta x_i(t)\|$ , respectively. The Lyapunov exponent ( $\lambda_i$ ) is a measure of how the distance between two points changes logarithmically with time.

$$\lambda_i = \lim_{t \rightarrow \infty} \frac{1}{t} \log_2 \frac{\|\delta x_i(t)\|}{\|\delta x_i(0)\|} \quad (7)$$

The Power Spectral Density (PSD) represents the distribution of the signal frequency components. In this study, PSD of each channel was estimated using Welch's method. Then we calculated the integral of the spectra from the beginning up to the peak and defined this as A1; we calculated the integral of the right spectra and defined this as A2 (Figure 4) [40]. Several ratios of PSD curve were included as features including: i) the maximum power (pmax) of the signal, ii) the frequency value at maximum power (Fmax), iii) the ratio of A1 to A2 (A1/A2), iv) A1/(A1+A2), and v) A2/(A1+A2).

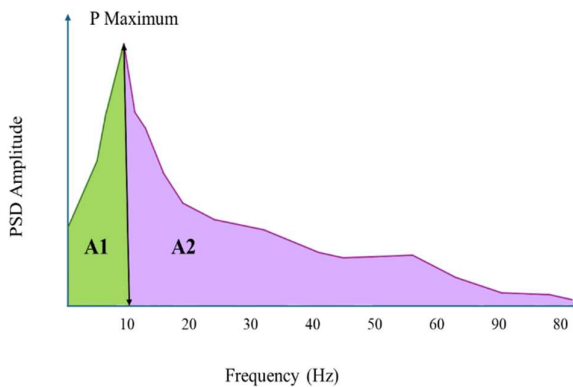


**Figure 4.** Power Spectral Density (PSD) graph.

#### 2.4.2. fNIRS Signal Processing:

fNIRS signal processing was performed using the SPM-fNIRS toolbox [42]. Raw fNIRS light intensity data were converted into HbO and HbR concentration changes using the modified Beer-Lambert law [43]. Saturated channels were

identified and excluded from the study. Long-distance channels measure hemoglobin concentration changes in the cortex, whereas short-distance channels measure activation in the extracerebral regions that are considered as noise [44]. In this study, measurements from the short-distance channels were eliminated from the observed fNIRS using a regression method [45]. Motion artifacts were removed from the HbO and HbR signals using the MARA algorithm [46]. A band-stop filter with cut-off frequencies of 0.1 and 2 Hz was applied to remove physiological noise. The HbO and HbR signals were then analyzed using the general linear model (GLM). The GLM model is presented in Eq. 8 [47]:

$$Y = X\beta + \varepsilon \quad (8)$$

Where Y is the fNIRS signal obtained as a result of signal processing, X is the design matrix,  $\varepsilon$  is the error and  $\beta$  is the weight values. In this study,  $\beta$  weights for HbO, HbR and total hemoglobin (HbT) for 16 fNIRS optodes were obtained after GLM analysis and these values were utilized for group comparisons.

#### 2.5. Statistical analysis:

All statistical analyses were conducted using SPSS 22.0 for Windows software (SPSS Inc., Chicago, IL). The features derived from EEG and fNIRS system were compared between the incongruent and neutral stimuli using a two-tailed paired t-test with a statistical threshold of 0.05. Statistical analyses were conducted for each EEG sub-band, resulting in 133 features (97 were from EEG and 36 were from fNIRS) that were found to be significantly different for incongruent and neutral stimuli.

fNIRS related features were evaluated to investigate differences in Stroop interference effect in three subregions of the PFC (DLPFC: Dorsolateral Prefrontal Cortex, dmPFC: Dorsomedial Prefrontal Cortex, FPPFC: Frontopolar Prefrontal Cortex). Besides neuroimaging biomarkers of the Stroop

interference effect, behavioral parameters were also evaluated. Reaction time and task errors were calculated automatically and averaged across all trials for each stimuli type.

### 2.6. Multilayer perceptron

MLP is a widely used classification technique that utilizes one or more hidden layers consisting of artificial neurons which are structures that aggregate inputs within a specific layer and generate an output via an activation function. With one or more neurons artificial neural networks can be characterized. MLP is a feed forward network, which has only forward connection, information flows forwardly manner. In neural network is finding optimal solution for diverse types of problems based on weights. For tuning weights MLP uses generally backpropagation algorithm uses derivate from output layer to input layer [48, 49].

For each neuron in an MLP, the input is defined as follows:  $y_i^h$  represents the output of a neuron in the previous layer,  $w_{ji}^h$  denotes the connection weight between the relevant neuron and the neuron under consideration.  $\theta_j^{h+1}$ , signifies the threshold value of the relevant neuron:

$$\begin{aligned}
 x_j^{h+1} &= \sum_i y_i^h w_{ji}^h - \theta_j^{h+1} \tag{9}
 \end{aligned}$$

Activation functions: The sigmoid function was utilized for the neurons. This choice ensures that incoming data exhibits proximal effects within defined intervals. No activation process is applied to the input layer. Normalization was performed for all features due to their diversity before classification was conducted.

$$\begin{aligned}
 y_j^0 &= x_j^0 \\
 y_j^h &= \frac{1}{1 + e^{-x_j^h}} \tag{10}
 \end{aligned}$$

The error term corresponding to the weight vector provided is calculated based on the

expected outcomes when progressing from input to output and obtaining results. Generally, this is quantified as the error's Least Mean Squares (LMS), and its formula is shown below.  $y_{j,c}^H(w)$  is output obtained for given weights and  $d_{j,c}$  is the desired output:

$$\begin{aligned}
 E(w) &= \frac{1}{2} \sum_{j,c} (y_{j,c}^H(w) - d_{j,c})^2 \tag{11}
 \end{aligned}$$

Backpropagation-based algorithms were employed to determine weights. As weights propagate in a chain to influence the output, their changes can also be regarded as a chain of derivatives (as depicted in the initial formula). Optimization of parameters are calculated in a backward manner, from output to input layers. At Eq. 13,  $hdec$  denotes the learning rate, typically ranging between 0.01 and 0.  $\epsilon$  represents a positive coefficient defining decay, and  $\alpha$  signifies momentum, typically ranging between 0 and 1.

$$\begin{aligned}
 \frac{\partial E}{\partial w_{ji}} &= \frac{\partial E}{\partial y_j} \frac{\partial y_j}{\partial x_j} \frac{\partial x_j}{\partial w_{ji}} \tag{12}
 \end{aligned}$$

$$\begin{aligned}
 \Delta w_{ji}^h(t) &= -\epsilon \frac{\partial E}{\partial w_{ji}} + \alpha \Delta w_{ji}^h(t-1) - hdec \\
 &\cdot w_{ji}^h(t-1) \tag{13}
 \end{aligned}$$

In this study, MLP was implemented using the Waikato Environment to Knowledge Analysis (WEKA) software [50]. The learning rate and momentum were tested within the range of 0.1 to 1 to achieve the highest classification accuracy. Through these trials, the learning rate was set to



0.3 (Figure 5), and the momentum value was determined to be 0.2 (Figure 6). The hidden layer contained 68 neurons, with the sigmoid function applied to these neurons (Figure 7). A 10-fold cross-validation was used for evaluation.

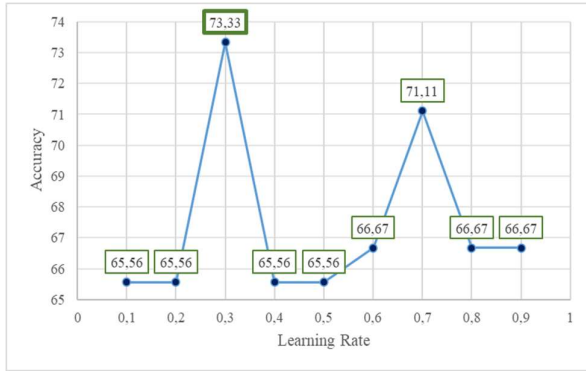


**Figure 5.** Accuracy rate depending on the learning rate.

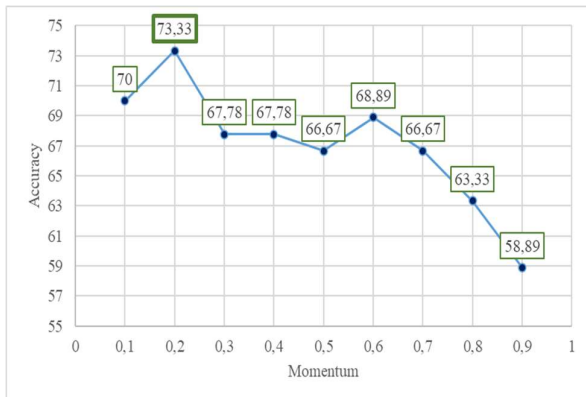


**Figure 6.** Accuracy rate depending on the momentum values.

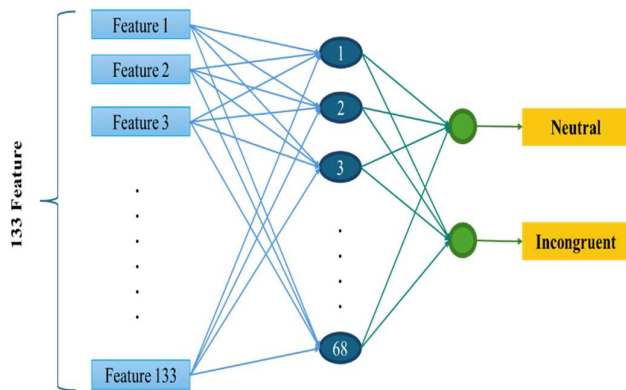


**Figure 7.** MLP model topology in this study.

### 3. Results

#### 3.1. Behavioral Performance:

Reaction time, the number of correct responses, and omission errors were compared between incongruent and neutral stimuli using paired samples t-tests. The mean reaction time for incongruent stimuli was  $950 \pm 115$  ms, whereas for neutral stimuli, it was  $880 \pm 108$  ms (Table 2). Incongruent reaction times were significantly longer than neutral ones ( $p < 0.01$ ). Number of correct responses was significantly higher for neutral stimuli ( $p < 0.01$ ). The number of omission errors was also higher for incongruent stimuli than neutral stimuli ( $p < 0.01$ ).

**Table 2.** Behavioral performance.

Parameters		Mean	Std D.	t	p
RT (ms)	neutral	879.99	107.98	-10.7	0.000
	incongruent	949.99	115.30		
Correct Response	neutral	47.40	2.10	3.82	0.000
	incongruent	45.49	3.46		
Omissions Error	neutral	0.91	1.12	-4.01	0.000
	incongruent	1.67	1.46		

RT: Reaction Time, Std D.: Standard Deviation

#### 3.2. EEG Findings:

In this study, EEG signals obtained from 17 channels were decomposed into five frequency sub-bands (gamma, beta, alpha, theta, delta) using wavelet transform, and linear-nonlinear features of each sub-band were investigated to explore differences between Stroop stimulus types. Statistically noteworthy features for incongruent and neutral stimuli are presented in Table 3 for each EEG channel ( $p < 0,05$ ). In particular, the fractal dimension emerged as a discriminative feature across several sub-bands, as seen in Table 3.

**Table 3.** EEG features.

EEG Locations	Gamma	Beta	Alpha	Theta	Delta
F7	FD, std	FD, std	-	FD, std	FD
F3	FD	-	-	FD	FD
Fz	FD	-	-	FD	FD
F4	Mean	-	-	FD	FD, HE
F8	FD, std	-	-	FD	FD
C3	-	-	PSD_R1, PSD_R2, PSD_R3	FD	FD
Cz	-	HD.	-	LYP	FD
C4	-	-	PSD_R1, PSD_R2, PSD_R3	FD	HE
T3	FD, std LYP	-	-	FD	FD, std
T4	FD, std	FD, PSD_R1	-	Fmax, FD, maxP, PSD_R1, PSD_R2, PSD_R3, LYP, std	FD, std
T5	FD, std	FD	-	FD	FD, Skewness
T6	FD, std	Entropy, FD, Hlber, std	PSD_R1	FD, std	LYP
P3	FD	-	-	FD	FD
Pz	FD	Fmax, FD, maxP, PSD_R1, PSD_R2, PSD_R3	-	FD	FD
P4	-	HD.	PSD_R1, PSD_R2, PSD_R3	-	HE
O1	FD	-	LYP	-	-
O2	FD	FD	PSD_R1	-	-

FD: Fractal Dimensions, std: Standard Deviation, HE: Hurst Exponent, PSD\_R1:  $A1/A2$ , PSD\_R2:  $A1/(A1+A2)$ , PSD\_R3:  $A2/(A1+A2)$ , HD: Harmonic Distortion, Entropy: Shannon Entropy, Hlber: Hibert Entropy, maxP: Maximum Power, Fmax: Frequency at maximum power, LYP: Lyapunov Exponent.

**3.4. fNIRS Findings:**

In fNIRS, signals obtained from 16 long-distance channels were analyzed to investigate the brain’s hemodynamic response during neutral and incongruent stimuli. To investigate the region where the Stroop effect was most pronounced, a total of six ROI regions were determined [43]:

- ROI 1: (CH 1 to CH 4) left DLPFC
- ROI 2: (CHs 5,6) left dorsomedial PFC,
- ROI 3: (CHs 7,8) left fronto-polar cortex,
- ROI 4: (CHs 9,10) right fronto-polar cortex,
- ROI 5: (CHs 11, 12) right dorsomedial PFC
- ROI 6: (CH 13 to CH 16) right DLPFC

Beta weights, calculated from HbO signals during incongruent and neutral stimuli were averaged in six ROI regions and compared between groups. Table 4 shows that the Stroop effect was higher in the right PFC than in the left region in the whole PFC, but statistical significance was observed only in the right and left DLPFC. As seen in Fig. 8, the right DLPFC (CHs 13-16) revealed a statistically significant higher Stroop effect than the left DLPFC (CHs 1-4).

**3.5. Classification Result**

Linear and nonlinear EEG features were combined with fNIRS-based features and applied to MLP to classify the brain’s response to incongruent and congruent stimuli. Sensitivity, specificity, and accuracy values were 76%, 71% and 73.3%, respectively. The response operator characteristic (ROC) area was 0.701.

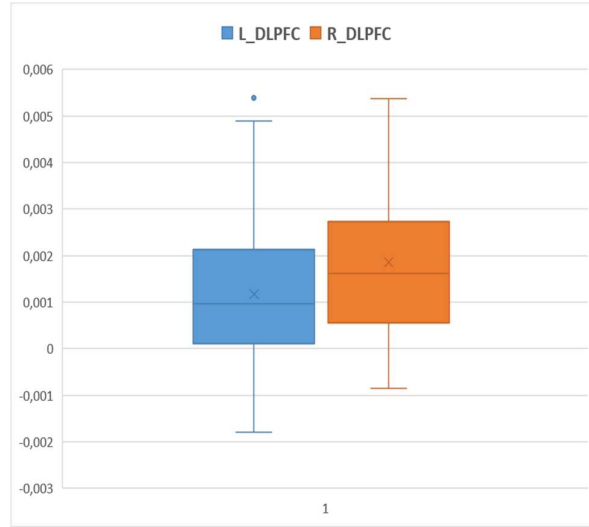


**Figure 8.** Boxplot graphs of the Stroop effect based on HbO beta values in the left DLPFC (L\_ DLPFC) and right DLPFC (R\_ DLPFC) regions.

**Table 4.** Analysis of the Stroop Effect in subregions of the PFC for right and left hemisphere.

<i>Stroop Interference Index (Incongruent-Neutral) HBO</i>	<i>Region</i>	<i>Mean</i>	<i>Std. Dev.</i>	<i>t</i>	<i>p</i>
<i>DLPFC</i>	Right	0.0018	0.0016	2.028	0.049
	Left	0.0012	0.0015		
<i>dmPFC</i>	Right	0.0025	0.0017	0.552	0.584
	Left	0.0023	0.0029		
<i>FPPFC</i>	Right	0.0035	0.0022	0.873	0.388
	Left	0.0031	0.0029		

*DLPFC: Dorsolateral Prefrontal Cortex, dmPFC: Dorsomedial Prefrontal Cortex, FPPFC: Frontopolar Prefrontal Cortex*

#### 4. Discussion

The present study aimed to comprehensively investigate the Stroop effect through concurrent EEG and fNIRS signals analysis using machine learning. For this purpose, various time-frequency features from different sub-bands of EEG signals and hemodynamic characteristics obtained from fNIRS signals were combined, and different Stroop stimuli were classified using machine learning algorithm. The study revealed that fractal dimension is associated with the Stroop interference effect across multiple EEG regions (Table 3). fNIRS results showed a pronounced manifestation of the Stroop effect, particularly in the right DLPFC. To our knowledge, this is the first study investigating the impact of Stroop interference via concurrent EEG/fNIRS system using a machine learning-based approach.

Reaction time and task errors to different stimuli in the Stroop task were evaluated in the study. Relative to neutral trials, significantly longer reaction times and increased task errors were observed in incongruent trials. Our behavioral data findings are consistent with previous studies demonstrating an interference effect of incongruent stimuli on individuals' cognitive performance [12, 51]. Similar to our results, Vamvakoussi et al. [52] observed longer reaction times and increased task errors in incongruent stimuli compared to neutral stimuli. These findings demonstrate an adverse effect of conflicting stimuli on cognitive processes.

Numerous EEG studies have investigated the Stroop effect, and most of these studies focused on ERP components. Stroop effect has been associated with decreased P3 amplitudes [53]. The present study aimed to investigate the Stroop effect via numerous linear and nonlinear EEG features. As shown in Table 3, the Stroop effect is mainly observed in the beta and theta bands.

Similarly, Hanslmayer et al. [15] associated increased Stroop interference with increased theta activity. Table 3 demonstrates that FD prominently reveals the Stroop effect, particularly in the gamma, beta, and theta bands. FD is a highly discriminative parameter in Stroop studies [54]. When examining regional activity, FD analysis revealed that the Stroop effect was most prominent in the frontal lobe. Regarding the specific features of PSD, the Stroop effect was predominantly observed in the alpha band, particularly in the central brain region. The study employed the GLM method, which has been commonly used recently in fNIRS signal analysis, to investigate the brain's hemodynamic activation during the Stroop test. All fNIRS optodes showed significantly greater HbO activation for incongruent stimuli than neutral stimuli ( $p < 0.05$ ). This result is consistent with studies associating the Stroop effect with increased PFC activation [9, 55, 56]. The study also investigated hemispheric differences in the Stroop effect by analyzing channels in the left and right PFC subregions. While the Stroop effect was observed in all PFC subregions ( $p < 0.05$ ), a significantly higher Stroop effect was observed in the right DLPFC region ( $p < 0.05$ ) (Table 5). This finding is in line with a study conducted by Friehs et al. [57] using repetitive transcranial magnetic stimulation (rTMS).

Combining different neuroimaging methods has recently become widespread in neuroscience studies, facilitating a comprehensive exploration of brain functions. This approach provides a comprehensive perspective on assessing brain functions through the complementarity of various methodologies, leading to enhanced success in classification studies. The study employed the multimodal EEG/fNIRS method, which has been demonstrated in numerous studies as complementary [58, 59]. With this method, the electroencephalographic and

hemodynamic responses of the brain to Stroop stimuli were evaluated simultaneously. Recently, Chen et al. [51] investigated the Stroop effect via ERP components and fNIRS using statistical methods, and they observed higher activation in the left DLPFC compared to the right in fNIRS. Furthermore, in a more recent study, Chen et al. [27] have employed EEG/fNIRS integration to elucidate the neural underpinnings of the perceptual conflict elicited by incongruent stimuli during the Stroop task, revealing a significant attenuation in neural activation.

In this current study, a machine learning approach was employed to evaluate the Stroop effect using multi-modal measurements for the first time in the literature. Features extracted from EEG and fNIRS signals were classified using MLP which is a widely used classifier for the physiological signals [60, 61]. The success rate of this classifier reached 73.3%, objectively demonstrating differential brain responses to incongruent and neutral stimuli.

#### **4.1. Conclusions**

The Stroop task, a milestone in cognitive neuroscience, has been widely used to explore the neural underpinnings of various cognitive functions, particularly those related to attention and cognitive control. The classic color-word interference paradigm is one of the most frequently used variant of Stroop test and involves different types of stimuli, challenging participants to manage conflicting information and thus providing valuable insights into cognitive processing. In this study, which represents the first investigation of the Stroop interference effect using different modalities and machine learning, it was observed that the electrophysiological and hemodynamic responses of the brain vary with different Stroop stimuli. Analyses demonstrated that increased activation in the PFC, particularly in the right DLPFC, was associated with the Stroop effect

compared to neutral stimuli. In this study, both linear and nonlinear features of EEG signals were extensively analyzed, with each EEG region being investigated in detail across different frequency ranges associated with the Stroop effect, thereby contributing new insights and features to the literature. In this study, the Stroop effect was evaluated using machine learning algorithms, providing a more objective approach to understanding cognitive processing. Additionally, using a homogeneous group has been particularly advantageous in minimizing the impact of individual differences on the significance of results obtained through these methods. Previous research has predominantly concentrated on the prefrontal cortex, a neural substrate crucial for cognitive functions. In contrast, our study employed an EEG system to capture brain activity from multiple regions, providing a more comprehensive view of the Stroop effect. The results demonstrate that the Stroop effect elicits significant activations across various brain areas. The Stroop task is commonly employed in studies comparing brain function between patients and controls. In this study, only healthy individuals were examined to investigate the functional operation of the Stroop effect objectively and comprehensively. The findings from this study, conducted with a healthy control group, provide valuable insights that could guide future research in neurological diseases and psychiatric disorders where the Stroop effect is frequently evaluated. Future studies could apply similar methodologies to examine this phenomenon in patient populations, further expanding our understanding of cognitive processing across different groups.

**Funding:** *This study was supported by Scientific and Technological Research Council of Turkey (TUBITAK) under the Grant Number 121E502 The authors thank to TUBITAK for their supports*

**Conflict of Interest:** Meltem İzzetoğlu has a small share in fNIRS Devices, LLC that produced the fNIRS system used in this work. The other authors declare that they have no conflicts of interest to report.

**Ethical Statement:** The ethical protocols were per the Helsinki Declaration and were approved by Erciyes University Clinical Research Ethics Committee with the number 2023/65. Informed consent was

**Acknowledgment:** We would like to thank the Proofreading & Editing Office of the Dean for Research at Erciyes University for copyediting and proofreading service for this manuscript.

### Open Access Statement

Experimental Biomedical Research is an open access journal and all content is freely available without charge to the user or his/her institution. This journal is licensed under a [Creative Commons Attribution 4.0 International License](#). Users are allowed to read, download, copy, distribute, print, search, or link to the full texts of the articles, or use them for any other lawful purpose, without asking prior permission from the publisher or the author.

**Copyright (c) 2024:** Author (s).

### References

- [1]Friedman NP, Trevor WR. The role of prefrontal cortex in cognitive control and executive function. *Neuropsychopharmacol.* 2022; (47): 72-89.
- [2]Daniel R, Radulescu A, Niv Y. Intact reinforcement learning but impaired attentional control during multidimensional probabilistic learning in older adults. *J Neurosci.* 2020; 40(5):1084-1096.
- [3]Shepherd J. Conscious cognitive effort in cognitive control. *Wiley Interdiscip. Rev Cogn.* 2023; 14(2): e1629.
- [4]Fleming LL, McDermott TJ, Cognitive Control and Neural Activity during Human Development: Evidence for Synaptic Pruning. *J Neurosci.* 2024; 44(26): e0373242024.
- [5]Stroop JR. Studies of interference in serial verbal reactions. *J Exp Psychol.* 1935;18(6):643.
- [6]Cattell JM. The time it takes to see and name objects. *Mind.* 1886;11(41):63-65.
- [7]MacLeod CM. Half a century of research on the Stroop effect: an integrative review. *Psychol Bull.* 1991;109(2):163.
- [8]Schroeter ML, Zysset S, Wahl M, et al. Prefrontal activation due to Stroop interference increases during development—an event-related fNIRS study. *Neuroimage.* 2004;23(4):1317-1325.
- [9]Huang Y, Su L, Ma Q. The Stroop effect: an activation likelihood estimation meta-analysis in healthy young adults. *Neurosci Lett.* 2020;716: 134683.
- [10]Kane MJ, Engle RW. Working-memory capacity and the control of attention: the contributions of goal neglect, response competition, and task set to Stroop interference. *J Exp Psychol Gen.* 2003;132(1):47.
- [11]Galer S, Op De Beeck M, Urbain C, et al. Investigating the neural correlates of the Stroop effect with magnetoencephalography. *Brain Topogr.* 2015;28:95-103.
- [12]Smith LL, Snyder HR, Hankin BL, et al. Composite Measures of Brain Activation Predict Individual Differences in Behavioral Stroop Interference. *J Cogn Neurosci.* 2023;35(5):781-801.
- [13]Lee DY, Seo EH, Yun JY, et al. Neural correlates of the stroop test performance in patients with Alzheimer’s disease: A FDG-PET study. *Alzheimer’s & Dementia.* 2011;7(4):7.



- [14] Ning R. How language proficiency influences stroop effect and reverse-stroop effect: A functional magnetic resonance imaging study. *J Neurolinguistics*. 2021; 60, 101027.
- [15] Hanslmayr S, Pastötter B, Bäuml KH et al. The electrophysiological dynamics of interference during the Stroop task. *J Cogn Neurosci*. 2008;20(2):215-225.
- [16] Song S, Zilverstand A, Song H, et al. The influence of emotional interference on cognitive control: A meta-analysis of neuroimaging studies using the emotional Stroop task. *Sci Rep*. 2017;7(1):2088.
- [17] Xu X, Deng ZY, Huang Q, et al. Prefrontal cortex-mediated executive function as assessed by Stroop task performance associates with weight loss among overweight and obese adolescents and young adults. *Behav. Brain Res*. 2017; 321:240-248.
- [18] Heidlmayr K, Kihlstedt M, Isel F. A review on the electroencephalography markers of Stroop executive control processes. *Brain and Cognition*. 2020;146:105637.
- [19] Chung RS, Cavaleri J, Sundaram S, et al. Understanding the Human Conflict Processing Network: A Review of the Literature on Direct Neural Recordings during Performance of a Modified Stroop Task. *Neurosci Res*. 2024; 206:1-19.
- [20] Sobhani V, Rezvani Z, Meftahi GH, et al. The Linear and Nonlinear Indices of Electroencephalography Change in the Stroop Color and Word Test. *J Mod Rehabil*. 2022;16(2):137-146.
- [21] Feng C, Becker B, Huang W, et al. Neural substrates of the emotion-word and emotional counting Stroop tasks in healthy and clinical populations: A meta-analysis of functional brain imaging studies. *NeuroImage*. 2018;173:258-274.
- [22] McKendrick R, Parasuraman R, Ayaz H. Wearable functional near infrared spectroscopy (fNIRS) and transcranial direct current stimulation (tDCS): expanding vistas for neurocognitive augmentation. *Front Syst Neurosci*. 2015; 9:9:27.
- [23] Muñoz V, Muñoz-Caracuel M, Angulo-Ruiz BY et al. Neurovascular coupling during auditory stimulation: event-related potentials and fNIRS hemodynamic. *Brain Struct. Funct*. 2023; 228(8), 1943-1961.
- [24] Masjoodi S, Fooladi M, Jalalvandi M, et al. Identification of the cognitive interference effect related to Stroop stimulation: using dynamic causal modeling of effective connectivity in functional Near-Infrared Spectroscopy (fNIRS). *JBPE*. 2020;10(4):467.
- [25] Altinkaynak M, Yeşilbaş D, Batbat T, et al. Multimodal Analysis of Cortical Activation in Young Male Adults with Internet Gaming Disorder: A Resting State EEG-fNIRS Study. *J Psychiatr Res*. 2024. 177: 368-377.
- [26] Li B, Li M, Xia J, et al. Hybrid Integrated Wearable Patch for Brain EEG-fNIRS Monitoring. *Sensors*. 2024;24(15):4847.
- [27] Chen Z, Gao C, Li T, et al. Open access dataset integrating EEG and fNIRS during Stroop tasks. *Sci Data*. 2023;10(1):618.
- [28] Zysset S, Müller K, Lohmann G, et al. Color-word matching stroop task: separating interference and response conflict. *Neuroimage*. 2001;13(1):29-36.
- [29] Schlögl A, Keinrath C, Zimmermann D, et al. A fully automated correction method of EOG artifacts in EEG recordings. *Clin Neurophysiol*. 2007;118(1):98-104.
- [30] Liu Y, Ayaz H, Shewokis PA. Multisubject “learning” for mental workload classification using concurrent EEG, fNIRS, and physiological measures. *Front Hum Neurosci*. 2017; (27);11:389.
- [31] Delorme A, Makeig S. EEGLAB: an open source toolbox for analysis of single-trial EEG

- dynamics including independent component analysis. *J Neurosci Methods*. 2004;134(1):9-21.
- [32] Urigüen JA, Garcia-Zapirain B. EEG artifact removal-state-of-the-art and guidelines. *J Neural Eng*. 2015; 12(3), 031001.
- [33] Jacob JE, Nair GK, Cherian A et al. Application of fractal dimension for EEG based diagnosis of encephalopathy. *Analog Integr Circ S*. 2019; 100, 429-436.
- [34] Amin HU, Malik AS, Ahmad RF, et al. Feature extraction and classification for EEG signals using wavelet transform and machine learning techniques. *Australas Phys Eng Sci Med*. 2015;38(1):139-149.
- [35] Liang Z, Wang Y, Sun X, et al. EEG entropy measures in anesthesia. *Front Comput Neurosci*. 2015;9:16.
- [36] Sinha N, Babu D. Statistical features based epileptic seizure EEG detection-an efficacy evaluation. *ICACCI, IEEE*. 2015:1394-1398.
- [37] Kimmatkar NV, Babu BV. Novel approach for emotion detection and stabilizing mental state by using machine learning techniques. *Computers*. 2021;10(3):37.
- [38] Blythe DA, Haufe S, Müller KR, et al. The effect of linear mixing in the EEG on Hurst exponent estimation. *NeuroImage*. 2014;99:377-387.
- [39] Übeyli ED, Güler İ. Detection of electrocardiographic changes in partial epileptic patients using Lyapunov exponents with multilayer perceptron neural networks. *Eng Appl Artif Intell*. 2004;17(6):567-576.
- [40] Güven A, Altınkaynak M, Dolu N, et al. Advanced analysis of auditory evoked potentials in hyperthyroid patients: The effect of filtering. *J Med Syst*. 2015;39:1-9.
- [41] Altıntop ÇG, Latifoğlu F, Akın AK, et al. Quantitative Electroencephalography Analysis for Improved Assessment of Consciousness Levels in Deep Coma Patients Using a Proposed Stimulus Stage. *Diagnostics*. 2023;13(8):1383.
- [42] Ye JC, Tak S, Jang KE, et al. NIRS-SPM: Statistical parametric mapping for near-infrared spectroscopy. *NeuroImage*. 2009;44(2):428-447.
- [43] Ayaz H, Izzetoglu M, Platek SM, et al. Registering fNIR data to brain surface image using MRI templates. *Conf Proc IEEE Eng Med Biol Soc*. 2006:2671-2674.
- [44] Gagnon L, Yücel MA, Boas D. et al. Further improvement in reducing superficial contamination in NIRS using double short separation measurements. *Neuroimage*. 2014;85:127-135.
- [45] Scholkmann F, Metz AJ, Wolf M. Measuring tissue hemodynamics and oxygenation by continuous-wave functional near-infrared spectroscopy—how robust are the different calculation methods against movement artifacts? *Physiol Meas*. 2014;35(4):717.
- [46] Scholkmann F, Spichtig S, Muehlemann T, et al. How to detect and reduce movement artifacts in near-infrared imaging using moving standard deviation and spline interpolation. *Physiol Meas*. 2010;31(5):649.
- [47] Perpetuini D, Russo EF, Cardone D, et al. Identification of functional cortical plasticity in children with cerebral palsy associated to robotic-assisted gait training: An fNIRS study. *J Clin Med*. 2022;11(22):6790.
- [48] Pal SK, Mitra S. Multilayer perceptron, fuzzy sets, classification. *IEEE Trans Neural Netw*. 1992; (3): 5, 683-697.
- [49] Almeida LB. In *Handbook of Neural Computation. Multilayer perceptrons*. IOP Publishing Ltd. and Oxford University Press, 1997.
- [50] Hall M, Frank E, Holmes G, et al. The WEKA data mining software: an update. *SIGKDD Explor Newsl*. 2009;11(1):10-18.

- [51] Chen Z, Ji X, Li T, et al. Lateralization difference in functional activity during Stroop tasks: a functional near-infrared spectroscopy and EEG simultaneous study. *Front Psychiatry*. 2023;14:1221381.
- [52] Vamvakoussi X, Van Dooren W, Verschaffel L. Naturally biased? In search for reaction time evidence for a natural number bias in adults. *J Math Behav*. 2012;31(3):344-355.
- [53] Wang W, Qi M, Gao H. An ERP investigation of the working memory stroop effect. *Neuropsychologia*. 2021;152:107752.
- [54] Abdul Hamid F, Saad MNM, Haris N. Comparison of Fractal Dimension and Wavelet Transform Methods in Classification of Stress State from EEG Signals. *IJCDS*. 2022;11(1):187-198.
- [55] Schroeter ML, Zysset S, Kupka T, et al. Near-infrared spectroscopy can detect brain activity during a color–word matching Stroop task in an event-related design. *Hum Brain Mapp*. 2002;17(1):61-71.
- [56] Egnér T, Etkin A, Gale S, et al. Dissociable Neural Systems Resolve Conflict from Emotional versus Nonemotional Distracters. *Cereb Cortex*. 2008;18(6):1475-1484.
- [57] Friebs MA, Klaus J, Singh T, et al. Perturbation of the right prefrontal cortex disrupts interference control. *NeuroImage*. 2020; 222:117279.
- [58] Güven A, Altinkaynak M, Dolu N, et al. Combining functional near-infrared spectroscopy and EEG measurements for the diagnosis of attention-deficit hyperactivity disorder. *Neural Comput & Applic*. 2020;32(12):8367-8380.
- [59] Alhudhaif A. An effective classification framework for brain-computer interface system design based on combining of fNIRS and EEG signals. *Peer J Comput Sci*. 2021;7:e537.
- [60] Safar AA, Salih DM, Murshid AM. Pattern recognition using the multi-layer perceptron (MLP) for medical disease: A survey. *Int J Nonlinear Anal. Appl*. 2023;14(1):1989-1998.
- [61] Singh P, Kansal M, Singh AP, et al. Real-Time Symptomatic Disease Predictor Using Multi-Layer Perceptron. In: *Future of AI in Medical Imaging*. IGI Global; 2024:155-167.